Materials Transactions, Vol. 55, No. 7 (2014) pp. 1045 to 1050
Special Issue on Laser Ultrasonics and Advanced Sensing 2013

Imaging Defects in a Plate with Full Non-Contact Scanning Laser Source Technique

Takahiro Hayashi*, Morimasa Murase, Natsuki Ogura and Tsunaji Kitayama

Toyota Central R&D Labs., Inc., Nagakute 480-1192, Japan

Previously, we used contact receiving transducers in the scanning laser source (SLS) technique for imaging defects on a plate in order to achieve a high signal-to-noise (SN) ratio. Herein, we developed a fast non-contact defect imaging technique that employs the SLS technique for in-line product inspection. Leaky Lamb waves from a plate were detected with a sufficiently large SN ratio by using low-frequency air-coupled transducers. Spurious images caused by reflected waves in the plate were removed by synthesizing images from multiple receivers. Defect images were compared for different repetition frequencies of laser emission. Images were found to be distorted at high repetition frequencies (2/3 kHz) owing to reverberations in the plate. [doi:10.2320/matertrans.I-M2014817]

(Received July 21, 2013; Accepted January 20, 2014; Published June 25, 2014)

Keywords: *laser ultrasonics, Lamb waves, imaging, non-contact evaluation, air-coupled ultrasonic transducer*

1. Introduction

The scanning laser source (SLS) technique is an inspection method for surface-breaking defects in bulk material[1–4] and inner defects in plates,[5–8] wherein an ultrasonic source generated by a laser is scanned over the surface of a material on which receiving transducers are fixed. A large number of waveforms acquired with this technique are converted into amplitude distributions, frequency change distributions,[1–3] and animations of ultrasonic wave propagation.[4] Although the receiving transducers are usually attached to the object at fixed positions to achieve a high signal-to-noise (SN) ratio, a concomitant drawback is that the contact reception limits application to untouchable materials. To apply the SLS technique to in-line inspection of products, a system that employs it must be capable of imaging the surfaces of products rapidly without contacting them. Therefore, in this work, we describe a fast non-contact defect imaging technique that employs an SLS.

Non-contact reception of ultrasonic waves can be performed by means of laser interferometers,[9] electromagnetic acoustic transducers (EMATs),[10] or air-coupled ultrasonic transducers,[11] although each method in principle has certain limitations. Laser interferometry, which requires reflected or scattered beams from the surface of an object, is strongly affected by the conditions of the surface, such as its inclination and roughness. EMATs, which work by the Lorentz force or magnetostrictive effect, can be applied only to electrical conductors or ferromagnetic materials below a lift-off of about 1 mm with low sensitivity. Air-coupled transducers, which have recently been developed in the high-frequency range beyond 100 kHz with high sensitivity, are still limited to a frequency range below about 1 MHz owing to the high attenuation in air.

We previously reported that the amplitude distributions measured with the SLS technique at very low frequencies correspond to the images of defects.[5–7] Focusing on this correspondence, here we investigate non-contact imaging by the SLS technique with air-coupled transducers in the low-frequency range. Moreover, by using the system developed here, we evaluated the effect of fast measurement on defect images in the range of repetition frequencies up to a few kilohertz.

2. Scanning Laser Source Technique for Plates and Use of Low-Frequency Air-Coupled Transducers as Receivers

Kromine *et al.*,[1] Fomitchov *et al.*,[2] Sohn *et al.*,[3] and Takatsubo *et al.*[4] showed that defects on the surface of a material could be detected by using the SLS technique to receive surface waves in the megahertz frequency range. In contrast, we have used the technique in the kilohertz (i.e., low) frequency range for imaging defects on the back surface of a plate.[5–8] In Refs. 5) and 6), we showed that the amplitude distribution obtained by the SLS technique corresponds to the thickness distribution for a plate with shallow rounded defects by using low frequencies below the A1 cut-off frequency. For notch-type defects, although distorted images were obtained owing to large reflections, synthesizing multiple images from more than one receiver produced enhanced defect images in which spurious images were reduced.[7] Subsequently, we demonstrated theoretically and experimentally that synthesizing multiple images from multiple receivers yields distinct images of notch-type defects in an aluminum plate at a frequency-thickness product range below about 200 kHz·mm.[8]

For aluminum plates 1 to 5 mm thick, this frequency range is very low compared with that of general ultrasonic inspection, e.g., below 40 to 200 kHz. Given that ultrasonic attenuation in air at such a low-frequency range is very small compared with that at a high-frequency range on the order of megahertz, non-contact reception with air-coupled transducers is practically feasible. In particular, air-coupled transducer generally used in ultrasonic distance meters, called open aperture-type air-coupled transducers as shown in Fig. 1(a), may be effective at frequencies below 100 kHz.

*Present address: Graduate School of Engineering, Kyoto University, Kyoto 615-8540, Japan

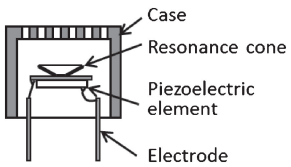

(a) 40 - kHz transducer

(Open aperture type transducer with a unimorph radial cone structure)

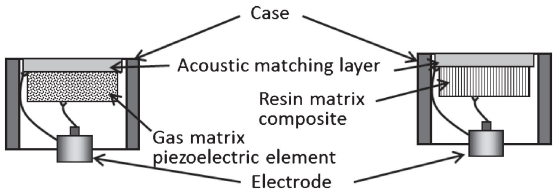

(b) 100 - kHz transducer

(Gas matrix composite transducer)

(c) 360 - kHz transducer

(Resin matrix composite transducer)

Fig. 1 Air-coupled transducers used in the experiments.

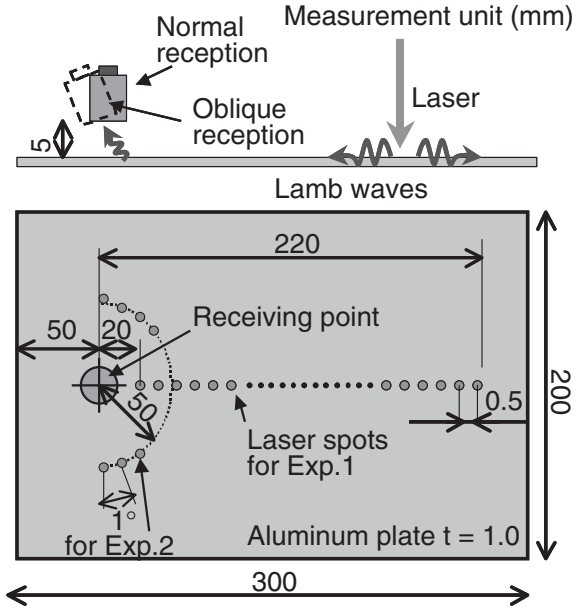

Fig. 2 Laser spots and receiving position in experiments to evaluate reception characteristics.

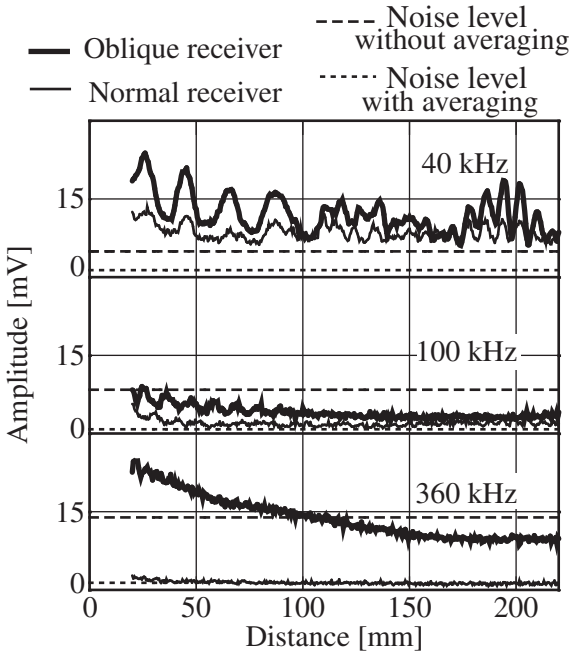

Fig. 3 Distance dependencies of amplitude for various air-coupled transducers.

3. Reception Characteristics of Various Air-Coupled Transducers

3.1 Measurements of ultrasonic leaky waves from a plate to the air

Firstly, to evaluate the reception characteristics of air-coupled transducers, leaked wave after propagating in an aluminum plate (200 mm × 300 mm × 1 mm) as Lamb waves were detected with three types of air-coupled transducers (central frequencies of 40, 100, and 360 kHz).

In experiments to investigate distance dependencies (Exp. 1), waveforms generated at laser spots on the center line of the plate were measured at the fixed receiving point shown in Fig. 2. Scanning with laser spots was conducted in 0.5-mm steps between 20 and 220 mm from the receiving point. In experiments to examine the angular profiles (directivities) of the air-coupled transducers (Exp. 2), waveforms generated at laser spots on a half circle with a radius of 50 mm were measured in 1°-increments, as shown in Fig. 2.

The following three types of air-coupled ultrasonic transducers were used: an open aperture-type transducer with a unimorph radial cone structure (Japan ceramic co., ltd. R4008A1, 40-kHz central frequency), a gas matrix composite transducer (Ultran, NCG100-D50, 100-kHz central frequency), and a transducer of resin matrix composite (Japan probe co., ltd., AR-0.4K 14 × 20 N, 360-kHz central frequency). Hereafter these air-coupled transducers are called 40-, 100-, and 360-kHz transducers, respectively. The air-coupled transducers were located about 5 mm apart from the plate surface in normal and oblique positions (Fig. 2), where oblique angles were adjusted to maximize the signals. A Nd-YLF pulse laser (Photonics Industries Inc. DC150-1053m, 1053-nm wavelength, 2 mJ/pulse at 1 kHz, 10-kHz maximum repetition frequency), was used to generate ultrasonic waves. The received signals were amplified by 60 dB and recorded in PC memory through an A/D board, after which they were processed by performing signal averaging 100 times and by band-pass filtering. The cut-off frequencies of the band pass filters were 20–80, 80–120, and 300–400 kHz for the 40-, 100-, and 360-kHz transducers, respectively.

3.2 Distance dependencies

Figure 3 shows the experimental results for Exp. 1, namely, variations in the amplitude with traveling distance for various air-coupled transducers. The upper, middle, and lower panels show results for the 40-, 100-, and 360-kHz transducers, respectively. The bold and thin solid lines denote results for oblique and normal receivers, respectively. Peak values of background noise were measured when the laser was not emitted. The dotted and dashed lines show the peak values of a single waveform and the averaged waveform, respectively.

Firstly, the differences between oblique and normal reception were investigated. In all three cases, larger signals were detected with oblique reception. In particular, for the 360-kHz transducer, although signals from the plate were not detected in the normal position (almost the same level as that of noise with averaging), adjusting the transducer to a suitable angle yielded very large signals. This is because the wave front of the leaky Lamb wave is oblique with respect to the plate surface. As the wavelength decreased at higher frequencies, the amplitude significantly differed for different angles of the transducer, at 360 kHz. On the contrary, in the low frequency range of 40 kHz, as the wavelength in the air is about 8.5 mm, which is comparable to the aperture size of 10 mm, the signals are insensitive to receiving angle.

Next, variations in amplitude with distance were considered. In oblique reception with the 100- and 360-kHz transducers, large signals beyond the noise level without averaging were detected in the near field of the receiving transducer. As the distance increased, the amplitude rapidly decreased below the noise level. In contrast, the 40-kHz transducer detected waveforms beyond the noise level without averaging in both oblique and normal positions at any distance up to 220 mm. This implies that low-frequency air-coupled transducers such as the 40-kHz transducer can be used for non-contact imaging of a large area without precisely adjusting the receiving angle.

In Fig. 3, large wavy changes in amplitude were measured, especially in the low-frequency case (40 kHz). For example, four peaks from 20 to 100 mm and five peaks from 170 to 220 mm were seen in oblique reception. This is caused by interference between direct waves and reflected waves at the plate edges. In the low frequency case (40 kHz), substantial interference occurred owing to low attenuation in the plate. From these results, we infer that the 40-kHz transducer, the most sensitive of the three types of air-coupled transducers tested here, is greatly affected by reflections in a plate.

3.3 Directivities

To investigate the directivities of the three types of air-coupled transducer for oblique and normal reception, amplitude distributions were obtained for the laser spots arranged in a half circle (Fig. 2). Figure 4 shows the amplitude distributions, namely the angular profiles from 0 to 180° (the top of the half circle to the bottom in Fig. 2).

In both oblique and normal positions with the 40-kHz transducer, the amplitude remained higher than the noise level without averaging over the entire range of angles. This indicates that the low-frequency transducer can receive leaky Lamb waves omni-directionally with small variations in sensitivity. In contrast, in the normal position with the 100- or 360-kHz transducer, almost all amplitudes were below the noise level. In oblique reception, the signals were limited within about ±20° from 90°, which is the direction facing the transducer surface. Namely, air-coupled transducers with a high frequency range (i.e., 100 and 360 kHz) could detect signals in oblique positions. However, the directivity of the angled beam transducer may become a problem in the imaging technique.

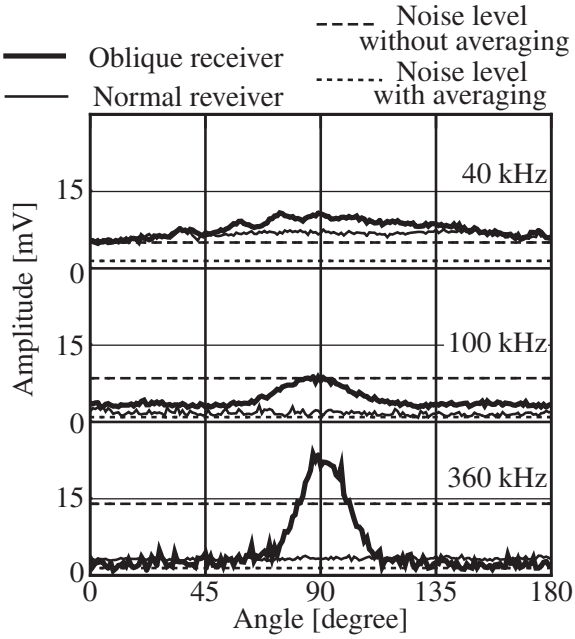

Fig. 4 Angular profiles (directivities) of various air-coupled transducers.

4. Imaging Experiments

Preferably, averaging should be avoided when imaging defects at high speed by using the SLS technique. In addition, to minimize positional variations in detectability, an air-coupled transducer is required to have constant sensitivity in all directions.

Considering the results in the previous section, the 40-kHz transducer in the normal receiving position satisfies all of these requirements. Therefore, in this section, non-contact imaging and its fast measurement system using the 40-kHz transducer were investigated.

4.1 Experimental setup for fast non-contact imaging

Figure 5 shows a schematic diagram of the experimental setup. In previous studies,[5–8] we recorded entire waveforms in all channels to a computer, and then detected peak values by using software. In this study, however, we produced analog peak detectors to realize high-speed defect imaging. The Nd-YLF laser used in the previous section was used as the pulsed laser for ultrasonic wave generation, and a GSI VM500 galvano mirror scanner provided trigger signals to synchronize the pulsed laser and peak detectors.

Ultrasonic waves generated by laser emission propagate along a plate as Lamb waves and leak to the air. The leaky waves were detected by eight 40-kHz transducers located at the four corners of a plate and the four midpoints between them, as shown in Fig. 5 (#1 to #8). The signals received by the eight transducers were amplified by 80 dB and filtered by a band-pass filter with 40-kHz central frequency. The peak detectors produce clock signals and peak hold signals within the time gate. Only the peak values were digitized by the A/D board.

The specimen used here was an aluminum plate of 200 mm × 300 mm × 1 mm with a straight, a zigzag, and a T-shaped notch 0.3 mm deep and 0.5 mm wide, each

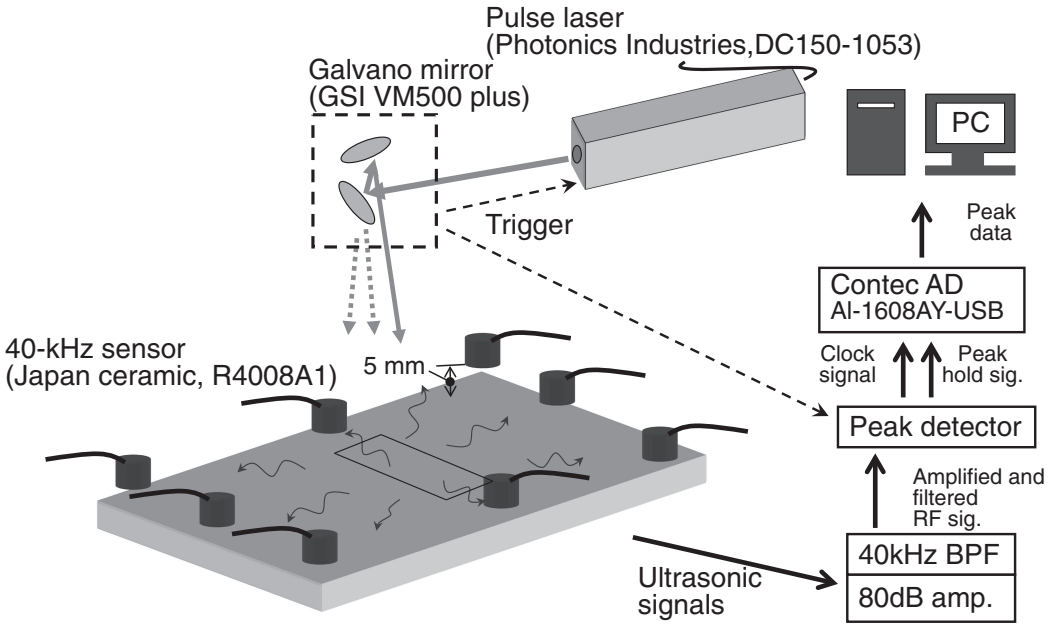

Fig. 5 Schematic diagram of experimental setup. A peak detector and a pulse laser equipment are started by trigger signals produced in Galvano mirror. A single peak data is transferred to PC at every pulse emission.

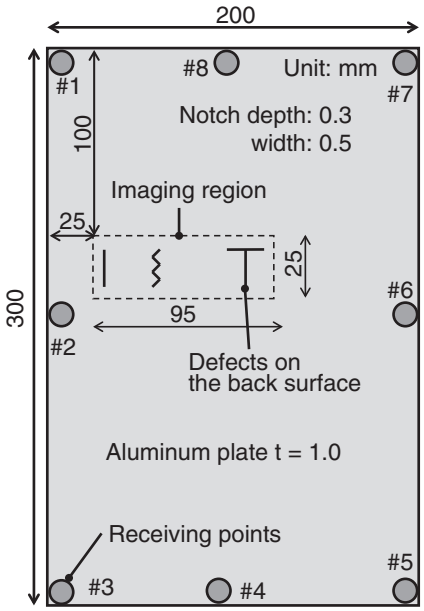

Fig. 6 Plate specimen used in the imaging experiments.

engraved on the back surface as shown in Fig. 6. The laser beam was scanned over an area of 25 mm × 95 mm, covering the defects in 0.5-mm steps with 9741 points (= 51 × 191).

4.2 Defect imaging

Figures 7(a)–7(h) show amplitude distributions created by taking peak values within the gate between 50 and 1000 μs for receivers #1 to #8, respectively. The repetition frequency of laser emission was 400 Hz. The defects in each amplitude distribution are unclear, and wavy spurious distributions caused by interference of reflected waves, similar to those in Fig. 3, appear throughout the images.

Figure 8(a) is a synthesized image created by summing the eight amplitude distributions of Figs. 7(a)–7(h). The wavy spurious patterns were reduced in the synthesized image because they were different in each amplitude distribution image. Moreover, defects were enhanced in the synthesized image because the defect regions appeared at the same place in each amplitude distribution.

Figure 8(b) shows images of defects obtained by using the 360-kHz transducers in oblique positions for comparison. In this measurement, transducers located at the same eight positions and all transducer surfaces faced the center of the plate at the appropriate oblique angle. The defect images in Fig. 8(b) were highly obscure compared to those in Fig. 8(a), and a dark area was seen between the zigzag and T-shaped defects, on which the beam paths of transducers #1 and #8 is located. The dark area is caused by the directivity of these transducers. All 360-kHz transducers in oblique positions have sensitive bands along the normal direction of transducer plane that are the straight lines stretching to the center of the plate. In the imaging region, as the sensitive bands of #1 and #8 were located between the zigzag and T shaped defects, the darker bands appeared when using the 360-kHz transducers in oblique positions. By contrast, defect images were not obtained owing to the small SN ratio with the 100- and 360-kHz transducers in the normal condition.

In the experiments performed above, the defect images obtained with the 40-kHz transducer were more distinct than those obtained by other means. The factors that are important for obtaining distinct images may be summarized as follows.

(1) The ability to acquire waveforms from a specimen at a low range of frequencies with a high SN ratio owing to the low attenuation in air (as shown in the experiments in the previous section).

(2) The effectiveness of defect imaging with the SLS technique at a low frequency-thickness product range, as demonstrated in a previous study.[8)]

(3) The reduction of spurious images due to reflections in a plate by synthesizing images from multiple transducers.

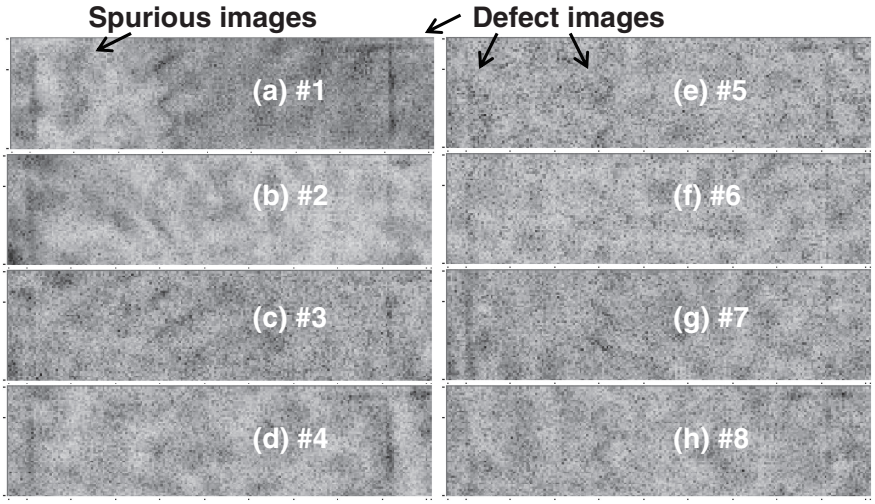

Fig. 7 Defect images of 40-kHz normal receivers at each position.

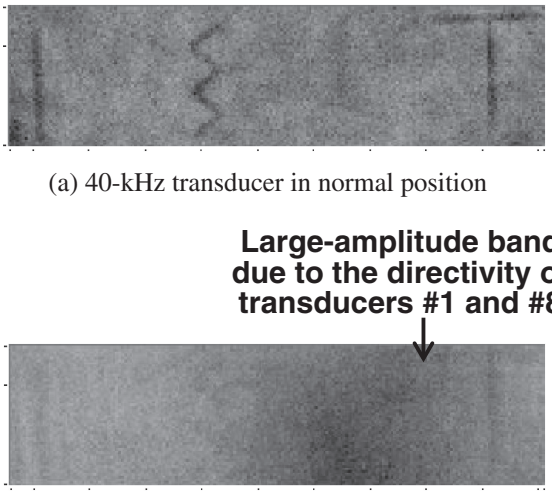

(a) 40-kHz transducer in normal position

(b) 360-kHz transducer in oblique position

Fig. 8 Synthesized defect images. (Summation of amplitude distributions obtained at eight transducers.)

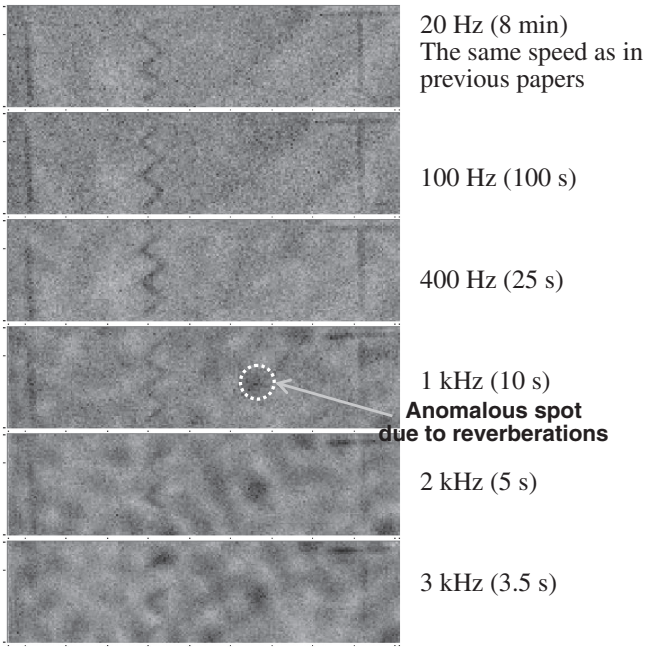

Fig. 9 Defect images for different repetition rates of laser pulse emission.

4.3 Influence of scanning speed on defect images

The pulsed laser equipment used here can emit laser pulses at the repetition frequencies ranging from DC to 10 kHz. As the repetition frequency is increased, the scanning speed and imaging speed increase. In this section, we examined the influence of scanning speed on defect images by varying the repetition frequency (six frequencies from 20 Hz to 3 kHz).

Figure 9 shows the synthesized images for different repetition frequencies with a signal gate of 50 to 200 μs. The required scanning (imaging) time was about 8 min at 20 Hz, which is the repetition frequency used in our previous studies. Although the imaging speed linearly decreased as the repetition frequency increased, more anomalous spots (enclosed by the white dotted circle in Fig. 9) appeared in the images. Up to 1 kHz, the straight, zigzag and T shape defects can be identified in the figures. However, the shapes of these defects become unclear at 2 and 3 kHz because of the numerous anomalous spots.

At high repetition frequencies, reverberations generated by the previous laser pulse were superposed on the present waveforms. The anomalous spots are caused by these large reverberations in the plate.

5. Conclusions

In this study, we investigated fast non-contact defect imaging by the scanning laser source technique with air-coupled transducers. In measurements of leaky Lamb waves by using three different air-coupled transducers with central frequencies of 40, 100, and 360 kHz, good signals were detected by the 40-kHz transducer in both oblique and normal positions. Moreover, distinct defect images were obtained by non-contact measurements with the 40-kHz transducers at eight positions and by synthesizing the eight images. Finally, defect images obtained at different repetition frequencies of laser pulse emission were compared. The shapes of the defects were clearly identified up to 1-kHz repetition frequency, which resulted in a scanning time

(imaging time) of about 10 s for 9741 raster points. At high repetition frequencies beyond 1 kHz, the resulting images were largely distorted owing to the superposition of ultrasonic waves generated by previous laser shots (i.e., reverberations) in the plate.

We suggest that more than eight air-coupled transducers can reduce spurious images caused by interference of reflected waves and reverberations at high repetition frequencies. An inspection system that uses multiple air-coupled transducers with a central frequency of 40 kHz also has a great advantage in price because the 40-kHz transducers generally used in ultrasonic distance meters are far less expensive than other types of air-coupled transducers.

REFERENCES

1) A. K. Kromine, P. A. Fomitchov, S. Krishnaswamy and J. D. Achenbach: Mater. Eval. **58** (2000) 173–177.
2) P. A. Fomitchov, A. K. Kromine, Y. Sohn, S. Krishnaswamy and J. D. Achenbach: *Review of Progress in Quantitative Nondestructive Evaluation*, Vol. 21, (Plenum publishing corporation, New York, 2002) pp. 356–362.
3) Y. Sohn and S. Krishnaswamy: J. Acoust. Soc. Am. **115** (2004) 172–181.
4) J. Takatsubo, B. Wang, H. Tsuda and N. Toyama: J. Solid Mech. Mater. Eng. **1** (2007) 1405–1411.
5) T. Hayashi, M. Murase and M. N. Salim: J. Acoust. Soc. Am. **126** (2009) 1101–1106.
6) M. N. Salim, T. Hayashi, M. Murase, T. Ito and S. Kamiya: *Review of Progress in Quantitative Nondestructive Evaluation*, Vol. 29, (Plenum publishing corporation, New York, 2010) pp. 231–238.
7) T. Hayashi, M. Murase and T. Kitayama: *Review of Progress in Quantitative Nondestructive Evaluation*, Vol. 30, (Plenum publishing corporation, New York, 2011) pp. 713–719.
8) T. Hayashi, M. Murase and T. Kitayama: Ultrasonics **52** (2012) 636–642.
9) C. B. Scruby and L. E. Drain: *Laser Ultrasonics: Techniques and Applications*, (Adam Hilger, New York, 1990).
10) M. Hirao and H. Ogi: *EMATs for Science and Industry: Noncontacting Ultrasonic Measurements*, (Kluwer-Academic, Boston, 2003).
11) D. A. Hutchins, W. M. D. Wright and D. W. Schindel: J. Acoust. Soc. Am. **96** (1994) 1634–1642.